Title
Modulation doping to control the high-density electron gas at a polar/non-polar oxide interface

Permalink
https://escholarship.org/uc/item/54z2311k

Journal
Applied Physics Letters, 101(11)

Author
Stemmer, Susanne

Publication Date
2012-09-13

Peer reviewed

Modulation doping to control the high-density electron gas at a polar/non-polar oxide interface

Tyler A. Cain, Pouya Moetakef, Clayton A. Jackson, and Susanne Stemmer[a)]
Materials Department, University of California, Santa Barbara, California 93106-5050, USA

A modulation-doping approach to control the carrier density of the high-density electron gas at a prototype polar/non-polar oxide interface is presented. It is shown that the carrier density of the electron gas at a $GdTiO_3/SrTiO_3$ interface can be reduced by up to 20% from its maximum value ($\sim 3 \times 10^{14}\,cm^{-2}$) by alloying the $GdTiO_3$ layer with Sr. The Seebeck coefficient of the two-dimensional electron gas increases concurrently with the decrease in its carrier density. The experimental results provide insight into the origin of charge carriers at oxide interfaces exhibiting a polar discontinuity. © *2012 American Institute of Physics*. [http://dx.doi.org/10.1063/1.4752439]

Interfaces such as Ge/GaAs,[1,2] $LaAlO_3/SrTiO_3$,[3] and $RTiO_3/SrTiO_3$,[4–6] where R is a trivalent rare earth ion, exhibit a polar discontinuity at the interface. An interfacial, high-density, mobile free electron (or hole) gas can serve to neutralize the divergent electrostatic potential energy created by the polar discontinuity. This mechanism is known as "electronic reconstruction." The origin of the free charge at $LaAlO_3/SrTiO_3$ interfaces has been a subject of significant debate in the literature.[7–9] One proposed explanation invokes electrons moving from the exposed polar surface of the $LaAlO_3$ to the interface.[10,11] Some support for this model is provided by the fact that mobile electrons are only observed when the $LaAlO_3$ layer exceeds a critical thickness.[12] This mechanism is similar to what is found in III-nitride heterostructures, where surface states are the source of free charge that compensates for built-in electric fields due to the discontinuity of a bulk polarization at the interface.[13] An exposed polar oxide surface has, however, a number of pathways available to solve its polar problem, including adsorbates and atomic reconstructions.[14] No dependence of the mobile carrier density on the thickness of the oxide layer with the exposed polar surface is expected in this case.[15] An alternative source of carriers, and mechanism to compensate for the polar problem, is *the interface itself*. Consider, for example, an atomically sharp $RTiO_3/SrTiO_3$ (001) interface, where the interface plane is TiO_2. The terminating $R^{+3}O^{-2}$ layer, which carries a +1 formal charge, can transfer ½ electron per interface unit cell, or $\sim 3 \times 10^{14}\,cm^{-2}$, to the interfacial TiO_2 plane, donating mobile charge to that layer. The mobile charge resides on one side of the interface (as determined by the band alignments) and will be attracted to the positive fixed charge at the interface, forming a confined two-dimensional electron gas (2DEG). For $RTiO_3/SrTiO_3$ interfaces, this description of interface charge appears to work well. In particular, independent of the individual layer thicknesses and growth sequences, a confined[16,17] 2DEG is consistently observed at $GdTiO_3/SrTiO_3$ interfaces. The 2DEG resides in the $SrTiO_3$ and has the required charge density, $\sim 3 \times 10^{14}\,cm^{-2}$.[6]

Further understanding of the origin of the mobile charge can be obtained by investigating the mobile charge density at polar/non-polar interfaces where the formal charges on the planes along the (001) surface normal deviate from the integer values of +1 and −1, respectively, in pure $LaAlO_3$ or $RTiO_3$. In this letter, we achieve this by alloying $Gd_{1-x}Sr_xTiO_3$ films and interfacing them with $SrTiO_3$. Stoichiometric $GdTiO_3$ is a prototype Mott insulator[18] and alloying with Sr results in hole doping. With an increasing amount of Sr (x), the polar problem, as well as the charge on the $Gd_{1-x}Sr_xO$ interface plane, is correspondingly reduced. One thus expects a proportional reduction in the mobile charge density. At $x \approx 0.20$, $Gd_{1-x}Sr_xTiO_3$ undergoes an insulator-to-metal transition,[19] which sets an upper limit for controlling the density of the 2DEG with this approach.

Films were grown by molecular beam epitaxy (MBE) on insulating (001) $(LaAlO_3)_{0.3}(Sr_2AlTaO_6)_{0.7}$ (LSAT) substrates by co-deposition from elemental and metal-organic sources.[20,21] The Sr content in the $Gd_{1-x}Sr_xTiO_3$ films was controlled through the Sr flux by adjusting the temperature of the Sr effusion cell, between 325 and 375 °C. X-ray photoelectron spectroscopy (XPS) was performed to estimate the Sr content. Ohmic contacts were 50 nm-Ti/300 nm-Au contacts, where Au is the top layer. Temperature dependent resistivity and Hall measurements were made using a physical properties measurement system (Quantum Design PPMS) in Van der Pauw geometry. Highly resistive $Gd_{1-x}Sr_xTiO_3$ films were measured in a rectangular geometry with a Keithley multimeter. In-plane Seebeck coefficient measurements[17] were made at room temperature. Two types of heterostructures were studied: $Gd_{1-x}Sr_xTiO_3$/LSAT and $Gd_{1-x}Sr_xTiO_3/SrTiO_3$/LSAT (see Table I).

Figure 1 shows the resistivity as a function of temperature for three $Gd_{1-x}Sr_xTiO_3$/LSAT samples with different x. While samples A1 ($x = 0$), A2, and A3 are insulating, the Sr content of A4 is sufficient for the film to be metallic (Fig. 1). The resistivity of the films decreases by more than three orders of magnitude (at room temperature) as x is increased. Hall measurements of A4 showed n-type behavior with a carrier concentration of $7.4 \times 10^{21}\,cm^{-3}$ at room temperature. The carrier concentration of metallic $R_{1-x}Sr_xTiO_3$ scales with x[22,23] and allows for estimating x to be about

[a)]Electronic mail: stemmer@mrl.ucsb.edu.

TABLE I. Summary of samples structures and estimated x.

Sample number	A1	A2	A3	A4	B1	B2	B3	B4
x (%)	0	4	13	44	0	4	13	44
SrTiO$_3$ thickness (nm)	–	–	–	–	65	65	65	65
Gd$_{1-x}$Sr$_x$TiO$_3$ thickness (nm)	11	22	22	22	3	11	11	11

0.44 for sample A4. Samples A1-A3 were too resistive for Hall measurements. The Sr content of A2 and A3 was estimated by extrapolating from the composition of A4, and the vapor pressure of sublimated Sr[24] at the Sr cell temperature, assuming that Sr incorporates in proportion to the amount evaporated (which is a reasonable assumption, see Ref. 21). The compositions are listed in Table I. For samples A2 and A3, XPS measurements were in reasonable agreement with these estimates, i.e., $x = 0.05$ and 0.11 for A2 and A3, compared to values of $x = 0.04$ and 0.13 estimated from the growth conditions.[25]

For the Gd$_{1-x}$Sr$_x$TiO$_3$/SrTiO$_3$/LSAT structures (B1-B4), the Gd$_{1-x}$Sr$_x$TiO$_3$ layers were grown under the conditions corresponding to those of A1-A4 (see Table I). Samples B1-B4 are metallic and *n*-type, even for Gd$_{1-x}$Sr$_x$TiO$_3$ layers where x was below the insulator-to-metal transition, due to the formation of the high-density 2DEG at the interface. The sheet resistances [Fig. 2(a)] of heterostructures with insulating Gd$_{1-x}$Sr$_x$TiO$_3$ layers (B1-B3) exhibit a large decrease with decreasing temperature, which is characteristic for transport in the SrTiO$_3$, due to its increasing mobility with decreasing temperature.[6] In contrast, the sheet resistance of the sample with the metallic Gd$_{1-x}$Sr$_x$TiO$_3$ layer (B4) is relatively temperature independent, consistent with being dominated by the metallic film. The carrier concentration of sample B4 is 5.10×10^{15} cm^{-2} at room temperature, more than an order of magnitude greater than samples B1-B3. The Hall resistance is linear in magnetic fields up to 7 T at all temperatures for all samples, indicating that the Hall coefficient is dominated by the *n*-type 2DEG for samples B1-B3. The mobility of Gd$_{1-x}$Sr$_x$TiO$_3$ is very low (0.57 cm^2 V^{-1}s^{-1} at room temperature for sample A4), typical for Mott materials, so carriers in

FIG. 2. Sheet resistance (a) and sheet carrier density (b) of Gd$_{1-x}$Sr$_x$TiO$_3$/SrTiO$_3$/LSAT heterostructures as a function of temperature.

the Gd$_{1-x}$Sr$_x$TiO$_3$ have little influence on the measured Hall coefficient.

Most importantly, the sheet resistances [Fig. 2(a)] and the carrier densities [Fig. 2(b)] of the 2DEGs in the Gd$_{1-x}$Sr$_x$TiO$_3$/SrTiO$_3$ heterostructures with insulating Gd$_{1-x}$Sr$_x$TiO$_3$ (B1-B3) change in proportion with the Sr concentration in the Gd$_{1-x}$Sr$_x$TiO$_3$ layer. At room temperature, the sheet carrier density of B1 ($x = 0$) is 3.12×10^{14} cm^{-2}, or approximately $\frac{1}{2}$ electron per interface unit cell. The sheet carrier densities of the 2DEGs in B2 and B3 are 2.72×10^{14} cm^{-2} and 2.50×10^{14} cm^{-2}, respectively, corresponding to a reduction in carrier density of 13% and 20% relative to sample B1. These results show that alloying of the Gd$_{1-x}$Sr$_x$TiO$_3$ films effectively modulates the density of the 2DEG. The low temperature (2 K) mobilities for these samples were between 279 and 425 cm^2 V^{-1} s^{-1}, sufficient to obtain Shubnikov-de Haas oscillations at high magnetic fields.[16] This modulation is also apparent in measurements of the thermopower (Seebeck coefficient), as discussed next.

Figure 3 shows the Seebeck coefficient of Gd$_{1-x}$Sr$_x$TiO$_3$/LSAT and Gd$_{1-x}$Sr$_x$TiO$_3$/SrTiO$_3$/LSAT heterostructures as a function of estimated x. The undoped GdTiO$_3$ film exhibits a positive (*p*-type) Seebeck coefficient of $+153$ μV/K, similar to bulk GdTiO$_3$.[26] The Seebeck
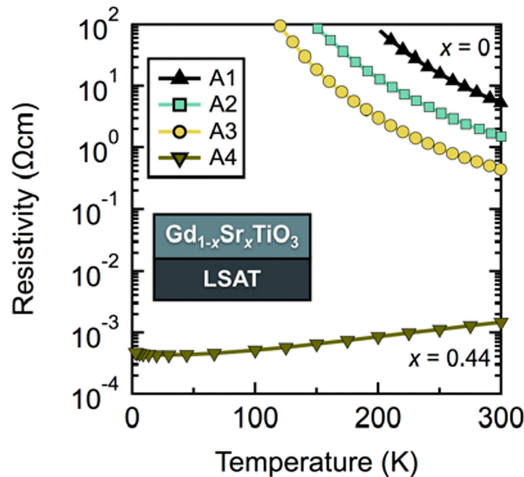

FIG. 1. Resistivity of Gd$_{1-x}$Sr$_x$TiO$_3$ thin films on LSAT as a function of temperature. For samples A1-A3, only every 20th measured data point is shown for clarity.
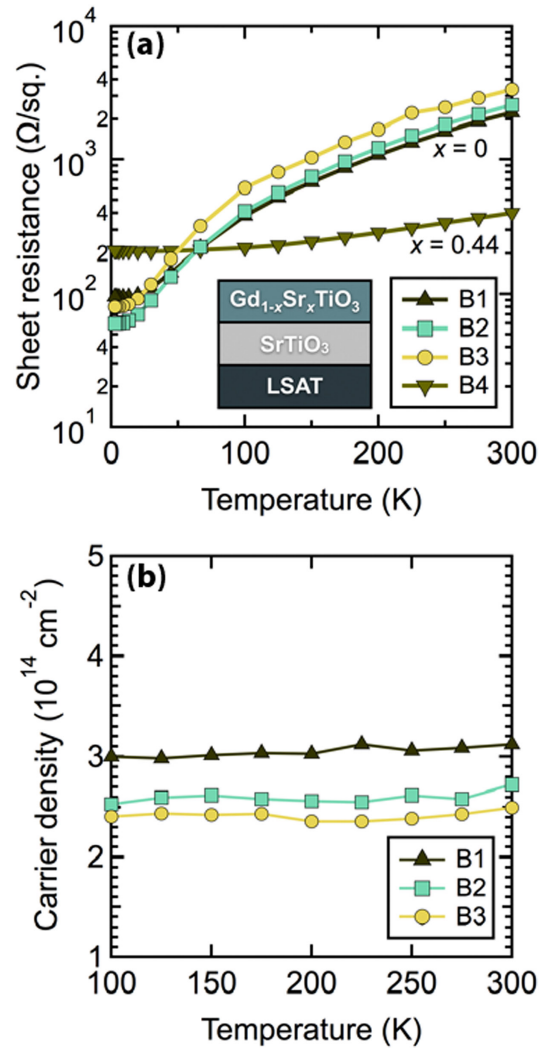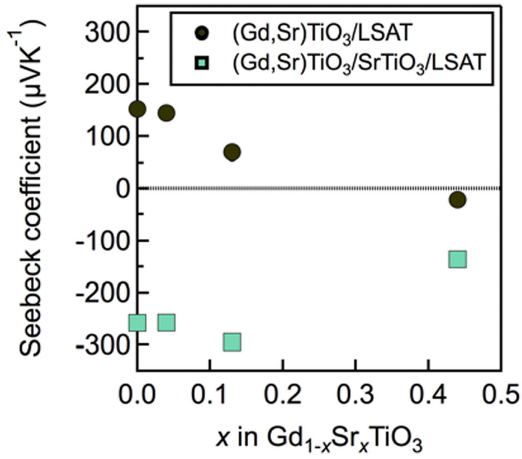
FIG. 3. Room temperature Seebeck coefficient of $Gd_{1-x}Sr_xTiO_3$/LSAT and $Gd_{1-x}Sr_xTiO_3$/SrTiO$_3$/LSAT heterostructures as a function of estimated Sr concentration, x.

coefficient decreases with increasing Sr content to $+145 \mu V/$K and $+69 \mu V/K$, for samples A2 and A3, respectively. The decrease is consistent with an increasing hole concentration.[27] The metallic sample (A4) has a negative Seebeck coefficient ($-22 \mu V/K$). The change in sign at the insulator-to-metal transition is typical of the rare earth titanates.[27]

Because the magnitude of the Seebeck coefficient decreases with increasing carrier concentration of the 2DEG,[17] one expects more negative values of the Seebeck coefficient of the 2DEG in the $Gd_{1-x}Sr_xTiO_3$/SrTiO$_3$/LSAT structures with increasing Sr concentration x. As seen in Fig. 3, this is indeed the case. The Seebeck coefficient increases in value from $-258 \mu V/K$ for samples B1 and B2 to $-295 \mu V/K$ for sample B3. We note that the Seebeck coefficient of samples B1-B3 is dominated by the 2DEG, due to its low resistivity. Specifically, for two parallel-connected layers (i.e., the 2DEG and the $Gd_{1-x}Sr_xTiO_3$, which are denoted by subscripts a and b), the measured Seebeck coefficient (S) is given by[28]

$$S = \frac{\frac{S_a}{R_{s,a}} + \frac{S_b}{R_{s,b}}}{\frac{1}{R_{s,a}} + \frac{1}{R_{s,b}}},\tag{1}$$

where $R_{s,i}$ is the sheet resistance of the layers. Because of the large difference in the sheet resistances (see Figs. 1 and 2), $S_a/R_{s,a}$ of the 2DEG is several orders of magnitude greater than $S_b/R_{s,b}$ of $Gd_{1-x}Sr_xTiO_3$. Thus, the $Gd_{1-x}Sr_xTiO_3$ layers do not contribute significantly to the measured S. The increase in magnitude of the Seebeck coefficient of sample B3 can therefore be attributed to the reduced 2DEG carrier density. The Seebeck coefficient of sample B4 is a composite of the metallic $Gd_{1-x}Sr_xTiO_3$ layer and the SrTiO$_3$ layer and thus more complicated to interpret in terms of the individual contributions.

In summary, measurements of the carrier densities and Seebeck coefficients of $Gd_{1-x}Sr_xTiO_3$/SrTiO$_3$ heterostructures show that reducing the polar discontinuity and fixed charge at the interface through alloying can be used to modulate the mobile carrier density in a high-density electron gas that forms at oxide interfaces exhibiting a polar discontinuity. The results shed light on the origin of the charge carriers at this interface.

As the fixed charge of the $(Gd_{1-x}Sr_xO)$ layer at the interface is reduced from its formal $+1$ value in pure GdO, the density of electrons donated to the d-band states of the interfacial TiO$_2$ layer is proportionally reduced. The experiments also show that the reduction in the 2DEG carrier density is somewhat greater than the estimated x, i.e., a 20% reduction in the 2DEG density for $x \approx 0.13$. The extra reduction may be attributed to other effects such as recombination with holes from the $Gd_{1-x}Sr_xTiO_3$ layer. Models of the mobile charge distribution and band bending obtained using a self consistent Poisson-Schrödinger solver[29] confirm that a modest additional reduction (relative to x) in the 2DEG density is expected. The results attest to the excellent control of charge densities that is possible with MBE grown layers. Finally, we note that the approach presented here can be considered as analogous to modulation doping, as developed for AlGaAs/GaAs interfaces.[30] Similar to AlGaAs/GaAs, the charge density in the 2DEG is modulated through doping of one of the layers comprising the interface. Here, the approach is used to reduce, rather than increase, the charge density.

[1]W. A. Harrison, E. A. Kraut, J. R. Waldrop, and R. W. Grant, Phys. Rev. B **18**, 4402 (1978).
[2]H. Kroemer, J. Cryst. Growth **81**, 193 (1987).
[3]A. Ohtomo and H. Y. Hwang, Nature **427**, 423 (2004).
[4]S. Okamoto and A. J. Millis, Nature **428**, 630 (2004).
[5]J. S. Kim, S. S. A. Seo, M. F. Chisholm, R. K. Kremer, H. U. Habermeier, B. Keimer, and H. N. Lee, Phys. Rev. B **82**, 201407 (2010).
[6]P. Moetakef, T. A. Cain, D. G. Ouellette, J. Y. Zhang, D. O. Klenov, A. Janotti, C. G. Van de Walle, S. Rajan, S. J. Allen, and S. Stemmer, Appl. Phys. Lett. **99**, 232116 (2011).
[7]S. A. Chambers, Surf. Sci. **605**, 1133 (2011).
[8]D. G. Schlom and J. Mannhart, Nature Mater. **10**, 168 (2011).
[9]M. Huijben, A. Brinkman, G. Koster, G. Rijnders, H. Hilgenkamp, and D. H. A. Blank, Adv. Mater. **21**, 1665 (2009).
[10]N. Nakagawa, H. Y. Hwang, and D. A. Muller, Nature Mater. **5**, 204 (2006).
[11]J. Mannhart and D. G. Schlom, Science **327**, 1607 (2010).
[12]S. Thiel, G. Hammerl, A. Schmehl, C. W. Schneider, and J. Mannhart, Science **313**, 1942 (2006).
[13]J. P. Ibbetson, P. T. Fini, K. D. Ness, S. P. DenBaars, J. S. Speck, and U. K. Mishra, Appl. Phys. Lett. **77**, 250 (2000).
[14]C. Noguera, J. Phys.: Condens. Matter **12**, R367 (2000).
[15]M. Stengel, Phys. Rev. Lett. **106**, 136803 (2011).
[16]P. Moetakef, D. G. Ouellette, J. R. Williams, S. J. Allen, L. Balents, D. Goldhaber-Gordon, and S. Stemmer, "Quantum oscillations from a two-dimensional electron gas at aMott/band insulator interface" (submitted).
[17]T. A. Cain, S. Lee, P. Moetakef, L. Balents, S. Stemmer, and S. J. Allen, Appl. Phys. Lett. **100**, 161601 (2012).
[18]H. D. Zhou and J. B. Goodenough, J. Phys.: Condens. Matter **17**, 7395 (2005).
[19]M. Heinrich, H. A. K. von Nidda, V. Fritsch, and A. Loidl, Phys. Rev. B **63**, 193103 (2001).

[20]B. Jalan, R. Engel-Herbert, N. J. Wright, and S. Stemmer, J. Vac. Sci. Technol. A **27**, 461 (2009).

[21]B. Jalan, P. Moetakef, and S. Stemmer, Appl. Phys. Lett. **95**, 032906 (2009).

[22]Y. Tokura, Y. Taguchi, Y. Okada, Y. Fujishima, T. Arima, K. Kumagai, and Y. Iye, Phys. Rev. Lett. **70**, 2126 (1993).

[23]T. Okuda, K. Nakanishi, S. Miyasaka, and Y. Tokura, Phys. Rev. B **63**, 113104 (2001).

[24]M. W. Chase, J. L. Curnutt, A. T. Hu, H. Prophet, A. N. Syverud, and L. C. Walker, J. Phys. Chem. Ref. Data **3**, 311 (1974).

[25]See supplementary material at http://dx.doi.org/10.1063/1.4752439 for the XPS data and the modelled charge density.

[26]G. V. Bazuev and G. P. Shveikin, Inorg. Mater. **14**, 201 (1978).

[27]C. C. Hays, J. S. Zhou, J. T. Markert, and J. B. Goodenough, Phys. Rev. B **60**, 10367 (1999).

[28]P. Pichanusakorn and P. Bandaru, Mater. Sci. Eng. R **67**, 19 (2010).

[29]M. Grundmann, "BandEng program" (unpublished).

[30]R. Dingle, H. L. Stormer, A. C. Gossard, and W. Wiegmann, Appl. Phys. Lett. **33**, 665 (1978).